Numerical investigation for convective heat transfer of nanofluid laminar flow inside a circular pipe by applying various models

FARQAD RASHEED SAEED[a*]
MARWAH ABDULKAREEM AL-DULAIMI

[a] Ministry of Science and Technology, Directorate of Materials Research, 55509 Al-Jadriya, Iraq

Abstract   The work presents a numerical investigation for the convective heat transfer of nanofluids under a laminar flow inside a straight tube. Different models applied to investigate the improvement in convective heat transfer, and Nusselt number in comparison with the experimental data. The impact of temperature dependence, temperature independence, and Brownian motion, was studied through the used models. In addition, temperature distribution and velocity field discussed through the presented models. Various concentrations of nanoparticles are used to explore the results of each equation with more precision. It was shown that achieving the solution through specific models could provide better consistency between obtained results and experimental data than the others.

Nomenclature

C_p	–	specific heat, J/kgK
$C_{p.bf}$	–	specific heat of the base fluid, J/kgK
$C_{p.nf}$	–	specific heat of the nanofluid, J/kgK
$C_{p.p}$	–	specific heat of the nanoparticles, J/kgK
D	–	pipe diameter, m

*Corresponding Author. Email: farqad.rasheed@gmail.com

d_p	–	nanoparticle diameter, m
d_{bf}	–	equivalent diameter of the base fluid molecule, m
h	–	heat transfer coefficient, $\text{W/m}^2\text{K}$
k_{bf}	–	thermal conductivity of base fluid, W/mK
k_{nf}	–	thermal conductivity of nanofluid, W/mK
k_p	–	thermal conductivity of nanoparticles, W/mK
M	–	molecular mass, kg/mol
N	–	Avogadro constant
Nu	–	Nusselt number
Pr	–	Prandtl number
q	–	heat flux, W/m^2
R	–	pipe radius, m
Re	–	Reynolds number
T	–	thermodynamic temperature, K
T_o	–	reference temperature, K
T_{fr}	–	freezing point of the base fluid, K
$\vec{v}$	–	velocity vector
V_x	–	velocity of the nanofluid, m/s
X	–	coordinate along the pipe axis, m

Greek symbols

κ	–	Boltzmann constant
μ_{bf}	–	dynamic viscosity of the base fluid, kg/m s
μ_{nf}	–	dynamic viscosity of the nanofluid, kg/m s
ρ_p	–	density of nanoparticles, kg/m^3
ρ_{bf}	–	density of the base fluid, kg/m^3
ρ_{nf}	–	density of the nanofluid, kg/m^3
ϕ	–	volume fraction of nanoparticles

Subscripts

bf	–	base fluid
nf	–	nanofluid
p	–	particles

1   Introduction

Heat exchangers have a primary role in contemporary technology, which motivates researchers to work on modifying their efficiency and heat exchanging performance. One of the drawbacks associated with heat exchangers is their working fluid that has a low thermal conductivity that attracted the interest of the researchers. With the appearance of a new generation of fluid suspensions represented by nanoparticles size, nanofluids found their way in heat exchangers. Many nanoparticles have been used

to prepare the nanofluids such as alumina Al_2O_3, copper oxide CuO, silica SiO_2, and titanium dioxide TiO_2 improved the thermal conductivity of the base fluid [1, 2]. One of the first studies was due to Masuda *et al.* [3] who performed dispersion of the ultra-fine particles into the fluid and inspected their heat transfer performance. However, the 'nanofluid' term did not exist yet. Later the term "nanofluid" began to be used, and the effective results of the nanofluid made it the focus of attention for the studies [4]. Experimental and numerical studies have been performed on the use of nanofluid and to characterize the influence of its thermophysical behavior and flow characteristic on the heat transfer performance [5, 6]. The convective heat transfer of nanofluids under laminar and turbulent flow was discussed by many studies. Pak *et al.* [7] introduced an experimental work on the impact of nanofluids on the convective heat transfer under turbulent flow condition which exhibited the increase in Nusselt number with the particle volume fraction; γ-Al_2O_3/water was used as a nanofluid. The increase in Reynolds number causes the increase in the Nusselt number also, while the results recorded a decrease in heat transfer coefficient by 3–12%. Presence of copper oxide CuO nanoparticles in the amount smaller than 1% volume fraction recorded an increase in the convective heat transfer coefficient of the base fluid (water) by 15%, as presented by Eastman [8]. Wen *et al.* [9] studied the behavior of Al_2O_3/water nanofluid at the entrance region of a tube under laminar flow condition. They found an improvement in local convective heat transfer coefficient by around 41% and 47% at Reynolds number equal to 1050 and 1600, respectively in comparison to the pure water. Many models were developed to describe the thermophysical properties of the nanofluids empirically. The classical Maxwell model that describes the nanofluid effective thermal conductivity developed by Vajjha *et al.* [10] to include the effect of Brownian motion as a function of temperature and volume fraction of nanoparticles. The modified model extracted through an experimental work performed testing of three types of nanoparticles aluminum oxide Al_2O_3, copper oxide CuO, and zinc oxide ZnO. The work recorded an enhancement in thermal conductivity with increasing the volume concentration of nanoparticles. The model was used later by the numerical study of Ebrahimnia *et al.* [11] to indicate the effective thermal conductivity of different nanofluids such as CuO/water and Al_2O_3/water. The work explores the effect of Brownian motion, and particle diameter using various volumes fraction of nanoparticles by applying the mentioned model and compared the results with experimental data. The results showed that the heat transfer coefficient improved

by the Brownian motion and has an inverse effect with the nanoparticle diameter. However, the convective heat transfer coefficient increased with nanoparticle concentration. The forced convection of laminar flow inside two different geometrical configurations was studied, numerically. The working nanofluids used in that work were water/γ–Al_2O_3 and ethylene glycol/γ–Al_2O_3, respectively. Effective thermal conductivity, dynamic viscosity, specific heat capacity, and density of the nanofluids were calculated across models independent of the variation in temperature [3,7,12,13]. The results indicate that the addition of nanoparticles augments the convective heat transfer coefficient, however, the ethylene glycol/γ–Al_2O_3 seems to have a better yield than water/γ–Al_2O_3 under the shear wall stress which result in drastic adverse effect as presented by Maiga *et al.* [14]. Corcione introduced an empirical correlation based on multi experimental data recorded by the studies [15]. The correlation applied for nanofluids to predict the effective thermal conductivity and dynamic viscosity. The equations were utilized with various nanoparticles concentration, diameters, and temperatures range. It was found that thermal conductivity augmented with the volume fraction of the nanoparticles and rising in temperature, while it decreased with the particle size of the nanoparticles. On the other hand, the same case was found for the dynamic viscosity in exception to the temperature effect that dynamic viscosity is independent on temperature. Onyiriuka *et al.* [16] studied the laminar and turbulent flow for nanofluids using a computational fluid dynamics (CFD). The geometry used in the simulation was a circular pipe. Both of three-two phase model, and a single-phase model, were applied in the presented work. It was noticed that a single-phase model deviated in 2% from the discrete phase model, in indication the local heat transfer coefficient that a discrete phase model recorded a 9% average deviation, under variable properties, and turbulent flow conditions. The discrete phase model can predict the local heat transfer coefficient with a 9% average deviation at variable properties, the single-phase model deviates 4.25% from the discrete phase model, under laminar flow conditions. Constant properties for the single-phase model give a better indication for the local heat transfer coefficient.

This paper presents a numerical study of laminar forced convection heat transfer inside a circular tube. Nanofluid is consisting of TiO_2 nanoparticles and water used as a working fluid, where the base fluid and nanoparticles are considered as a single phase. Four models are used to determine the most accurate results in comparison to the experimental data. Temperature-

dependent, independent of temperature, particle diameter, and Brownian motion are parameters included inside the models, to clarify their effect on the results accuracy.

2 Mathematical model

Single-phase flow is used in this work that both water and the nanoparticles are treated as a single phase with the variation in thermophysical properties of the nanofluid of such properties as thermal conductivity, dynamic viscosity, specific heat capacity, and density [6]. However, all the mentioned parameters are counted as effective properties according to specific equations. Different models are used to calculate the effective thermophysical properties that every model has a characteristic part like Brownian motion or particles diameters, and dependent or independent on the temperature. The dimensional governing equations that cover the single-phase flow at steady state are [17–19]:

continuity equation
$$\nabla \cdot (\rho_{nf}\vec{v}) = 0\,, \tag{1}$$

momentum equation
$$\nabla \cdot (\rho_{nf}\vec{v}\,\vec{v}) = -\nabla p + \nabla \cdot (\mu_{nf}\nabla\vec{v})\,, \tag{2}$$

energy equation
$$\nabla \cdot (\rho_{nf}\vec{v}C_pT) = (\nabla \cdot k_{nf}\nabla T)\,. \tag{3}$$

3 Thermophysical properties of nanofluids

Thermophysical properties of nanofluids were achieved by correlations suggested by the researches, which were based on the calculation of the nanofluid's effective properties. Judging from the fact that nanoparticles have a higher thermophysical properties such as thermal conductivity, the addition of nanoparticle's weight fraction improves the heat transfer coefficient of the base fluid water. However, the suggested models have a slight paradoxical among each other's, and with experimental data, that's why a survey of some essential models in comparison with experimental data of ex-work is considered [20].

4 Temperature-independent models

4.1 Model 1

In this model the equations

$$k_{nf} = k_{bf}\left(125.62\phi^2 + 4.82 + 1.0\right),\tag{4}$$

$$\mu_{nf} = \mu_{bf}\left(199.21\phi^2 + 4.62 + 1.0\right)\tag{5}$$

represented two correlations to evaluate the effective thermal conductivity and viscosity of nanofluid, which they are based on experimental measurements [20]. The model compared with experimental data which shows acceptable results.

4.2 Model 2

In this model the equations

$$\frac{k_{nf}}{k_{bf}} = (4.97\phi + 2.72\phi + 1.0),\tag{6}$$

$$\frac{\mu_{nf}}{\mu_{bf}} = \left(123\phi^2 + 7.3\phi + 1.0\right),\tag{7}$$

$$\rho_{nf} = (1 - \phi)\,\rho_{bf} + \phi\rho_p\,,\tag{8}$$

$$C_{p.nf} = (1 - \phi)\,C_{p.bf} + \phi C_{p.p}\tag{9}$$

together with two other correlations for achieving the effective thermal conductivity and viscosity at constant temperature which they found empirically [14]. Density and specific heat capacity were found using Eqs. (8), and (9) [21].

5 Temperature-dependent models

5.1 Model 3

The effective thermal conductivity correlation, originally offered by Koo *et al.* [22], then modified by Vajjha *et al.* [10], consists ofa static part according to the Maxwell theory and a dynamic part. The dynamic thermal conductivity part contains the effect of Brownian motion and particle diameter; it also includes the Boltzmann constant. The following equation is

accounting for the temperature dependent properties of the effective thermal conductivity of nanofluid:

$$k_{nf} = \left[\frac{k_p + 2k_{bf} - 2(k_{bf} - k_p)\phi}{k_p + 2k_{bf} + (k_f - k_p)\phi} \right] k_{bf}$$
$$+ \left(5 \times 10^4 \beta \phi \rho_{bf} C_{P.bf} \right) \times \sqrt{\frac{\kappa (T + 273.15)}{\rho_{bf} d_p} f(T, \phi)} , \qquad (10)$$

$$f(T, \phi) = \left(2.8217 \times 10^{-2} \phi + 3.917 \times 10^{-3} \right) \frac{T + 273.15}{T_o + 273.15}$$
$$- 3.0699 \times 10^{-2} \phi - 3.91123 \times 10^{-3} , \qquad (11)$$

$$\beta = 8.4407(100\phi)^{-1.07304} , \qquad (12)$$

where $f(T, \phi)$ is an empirical function based on the experimental data of the nanofluid, and β describes the volume of the liquid associated with the nanoparticles, accordingly. It decreases with increase of the nanoparticles volume fraction due to the effect of viscosity resulted from the movement of nanoparticles. The validity of this empirical correlation falls into the range $1\% \leq \phi \leq 10\%$ of Al_2O_3 concentration and temperature range 298 K $\leq$ $T \leq$ 363 K, and its validity for TiO_2 is indicated.

The nanofluid dynamic viscosity correlation is described by the following equation, which based on the experimental data of Kim *et al.* [23]

$$\mu_{nf} = \mu_{bf}(T)A \exp(B\phi) , \qquad (13)$$

where A and B are constants and $A = 0.9$, whereas $B = 10.0359$, and are determined from the experimental data of Kim *et al.* [23].The density and specific heat capacity as a function of temperature are described by the following equations:

$$\rho_{nf}(\phi, T) = (1 - \phi)\rho_{bf}(T) + \phi\rho_p , \qquad (14)$$

$$C_{p.nf}(\phi, T) = \frac{(1 - \phi)\rho_{bf}(T)C_{p.bf}(T) + \phi\rho_p C_{p.p}}{(1 - \phi)\rho_{bf}(T) + \phi\rho_p} . \qquad (15)$$

5.2   Model 4

Another two correlations for evaluating the thermal conductivity and dynamic viscosity of nanofluids was presented by Corcione [15]:

$$\frac{k_{nf}}{k_{bf}} = 1 + 4.4 Re^{0.4} Pr^{0.66} \left(\frac{T}{T_{fr}} \right)^{10} \left(\frac{k_p}{k_{bf}} \right)^{0.03} \phi^{0.66} , \qquad (16)$$

$$\frac{\mu_{nf}}{\mu_{bf}} = \frac{1}{1 - 34.87 \left(\dfrac{d_p}{d_{bf}}\right)^{-0.3} \phi^{1.03}} \, , \tag{17}$$

where

$$\text{Re} = \frac{\rho_{bf} u_B d_p}{\mu_{bf}} \, , \tag{18}$$

$$u_B = \frac{2\kappa T}{\pi \mu_{bf} d_p^2} \, . \tag{19}$$

The correlations are temperature-dependent and they account for the effect of nanoparticle diameter, besides the impact of nanoparticle volume concentration. The dynamic viscosity correlation includes the effect of equivalent diameter of the base fluid molecule:

$$d_{bf} = 0.1 \frac{(6M)^{1/3}}{N \pi \rho_{bf}} \, . \tag{20}$$

This parameter is included in such calculation for the first time. Also, a Boltzmann constant is included in the thermal conductivity model. The density and specific heat capacity as a function of temperature were found following Eqs. (14) and (15). Corcione model designed for oxides and metal nanoparticles in particle size range $10–150 \times 10^{-9}$ m, volume fraction 0.002–0.09, and temperature range 294–324 K.

6   Thermophysical properties of the base-fluid

The base fluid that used in the present work is water, so the polynomial thermophysical properties as a function of temperature, are selected from the simple curve fitting of water, which it is available in Mcnab *et al.* [24]:

$$\begin{aligned} \mu_{bf} = {} & 0.414092804247831 - 4.792184560427 \times 10^{-3}T \\ & + 2.0927097596 \times 10^{-5}T^2 - 4.0781184 \times 10^{-8}T^3 \\ & + 2.9885 \times 10^{-11}T^4 \, , \end{aligned} \tag{21}$$

$$\rho_{bf} = 765.33 + 1.8142T - 0.0035T^2 \, , \tag{22}$$

$$\begin{aligned} C_{P.bf} = {} & 10444.58656104 - 54.08920728T \\ & + 0.15359377T^2 - 0.00014301T^3 \, , \end{aligned} \tag{23}$$

$$k_{bf} = -0.46662403 + 0.00575419T - 7.18 \times 10^{-6}T^2 \, . \tag{24}$$

7   Numerical method and simulation

The domain used in the present work is a circular pipe of 2 m in length and 0.004 m in diameter, as shown in Fig. 1a, supplied with a constant heat flux 4000 W/m^2 following the experimental work of He *et al.* [20]. The suggested boundary condition of this work is a uniform velocity field at the inlet, and zero gradient is assumed at the outlet to all hydrodynamic variables, with no slip condition at the wall. The temperature that is applied at the inlet is 295 K, and the outlet temperature is employed as a constant temperature gradient. The commercial finite element analysis, solver anda general-purpose simulation software, Comsol Multiphysics [26], is used to solve the numerical procedure.
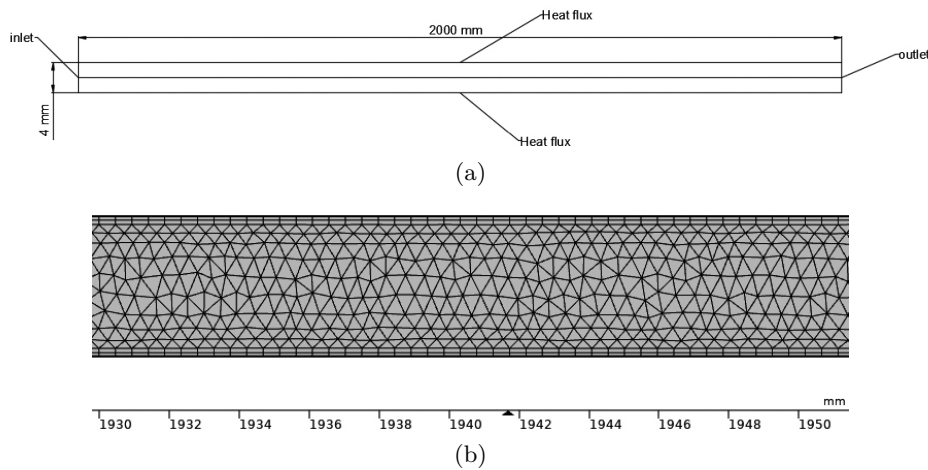
Figure 1: (a) Schematic representation for the used geometry, (b) mesh for the used model.

Coarse-mesh type of finite element is used in the simulation, the maximum element size is 899×10^{-3} m, while the minimum element size is 402×10^{-4} m. The maximum element growth rate is 1.2, curvature factor is 0.4, and resolution of narrow region is 1 (Fig. 1b).

8   Validity of the model

The validity of this simulation is achieved by finding the local heat transfer coefficient of water at various axial positions in comparison with the experimental and numerical data presented by He *et al.* [20], Fig. 2. Water flow

through a circular pipe supplied with a constant heat flux of 4000 W/m^2 under laminar conditions has been applied at Reynolds number 900. Local Nusselt number of water calculated at different axial positions was also compared with the experimental and numerical results of [20] and the outcomes of Shah equation [25] as shown in Fig. 3. A good agreement is achieved be-
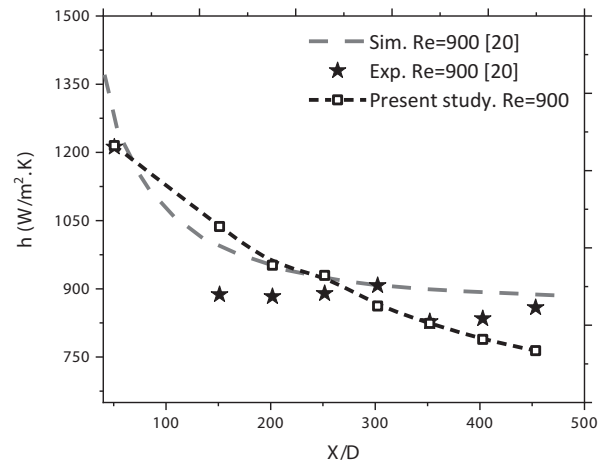
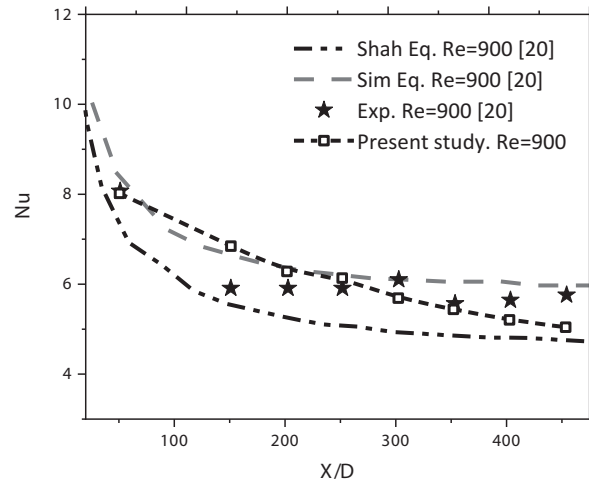Figure 2: The axial variation of heat transfer coefficient of the present study in comparison with literature data.

Figure 3: The axial variation of Nusselt number of the present study in comparison with literature data.

tween the presented study and experimental and numerical results as well as the Shah equation both in terms of heat transfer coefficient and Nusselt number. The standard deviation for the calculated heat transfer coefficient and Nusselt number is 8.17%, and 8.45%, respectively.

9   Results and discussion

9.1   Thermal conductivity and dynamic viscosity of nanofluid

The correlations of effective thermal conductivity and effective dynamic viscosity can consider the essential part, which dominates the thermal behavior of the nanofluid. Figure 4 presents the k_{nf}/k_{bf} ratio as a function to the nanoparticles volume fraction ϕ, evaluated at a constant temperature 295 K and calculated by the considered theoretical models and compared with experimental data. It can be noticed a good consistency of data to the experimental work recorded in [20] as the correlation due to He *et al.* represents the fit of the experimental work. The closest model after He *et al.* was the model due to Corcione [15], while the other models recorded more deviated data. The μ_{nf}/μ_{bf} ratio as a function of ϕ shown in Fig. 5 indicated a similar behavior to Fig. 4 in case of He *et al.* model. The other models shown another behavior, namely the data exhibit higher values of k_{nf}/k_{bf}
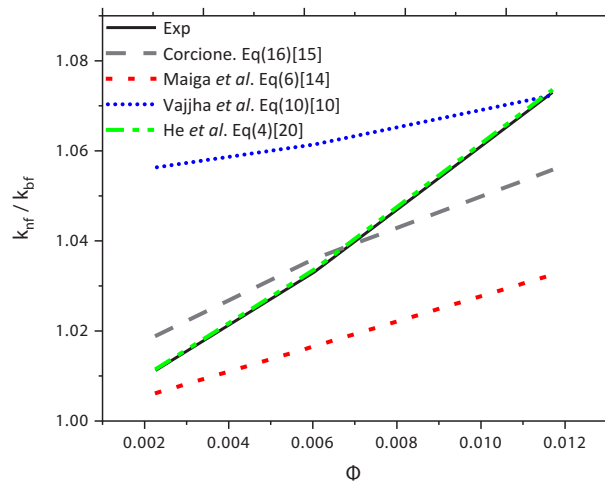

Figure 4: The k_{nf}/k_{bf} ratio as a function to the nanoparticles volume fraction ϕ.

than the experimental data and a lower values of μ_{nf}/μ_{bf} such as Vajjha *et al.* [10], while the Maiga *et al.* [14] model outputs show lower values of k_{nf}/k_{bf} than the experimental data and higher values of μ_{nf}/μ_{bf} than the experimental data. The obtained results are reasonable, that a high viscosity minimizes the thermal conductivity and *vice versa.*
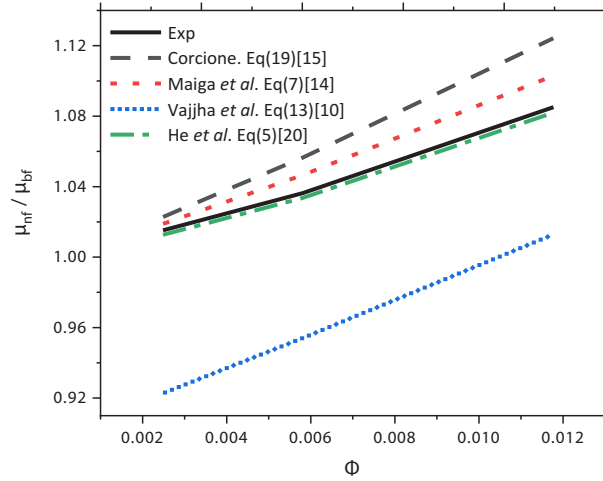

Figure 5: The μ_{nf}/μ_{bf} ratio as a function to the nanoparticles volume fraction ϕ.

9.2   Convection heat transfer coefficient as a function of the axial position

The values of convective heat transfer coefficient can be determined as shown in Figs. 6–9. They were evaluated at different axial positions by using two concentrations of nanoparticles, while the Reynolds number was fixed at 900. An improvement in the heat transfer coefficient along the axial position can be observed, from the mentioned figures as the volume fraction of nanoparticles increased. Moreover, the heat transfer coefficient was reduced toward the axial distance as it meant to be. Close results were found between the experimental and simulation for the water heat transfer coefficient, however, there was some deviation at some X/D positions, which can be interpreted by the uncertainty associated with each experimental work such as the perfect insulation around the heater or measuring tools that were used in the experiment.

9.3 The effect of nanoparticles addition

Nanoparticles addition improves the heat transfer coefficient of water as shown in Figs. 6–9, that the augmentation detected with increasing the nanoparticles concentration for the experimental and numerical results at Reynolds number of 900 [20]. All the considered models agreed in the mentioned improvement despite the difference in the recorded values [10,14,15], which will be discussed later.

Nusselt number exhibits a similar behavior such as the one found in the heat transfer coefficient, which is represented by increasing the Nusselt number with increasing the nanoparticles volume fraction along with the axial distance at Reynolds number 900 as shown in Figs. 10–13. The improvement in Nusselt number is recorded in the experimental work and for all the models used in [10, 14, 15]. However, the increasing percent in Nusselt number varied from one correlation to another one according to the used model, as it will discussed.

9.4 The behavior of heat transfer coefficient

In general, nanoparticles addition to the base fluid (water) improves the heat transfer coefficient at all axial positions. The impact of nanoparticles on the base fluid is evaluated according to four models in comparison to the experimental study [20]. The models expose the thermal behavior at a constant temperature (T), as a function of temperature, the effect of including the Brownian motion, and the influence of base fluid molecule size. As mentioned before, the heat transfer coefficient augmented due to addition of nanoparticles and with increasing the volume fraction of the nanoparticles, this result was found in all used models. However, the models showed paradoxical outcomes in comparison with experimental data, the closest result obtained with Maiga *et al.* [14] and Corcione [15] models, Figs. 7 and 9, which they exhibit 14.032%, 11.337%, and 15.957%, 12.719% at 1.18% and 0.60% volume fractions of nanoparticles, respectively, with standard deviation equal to 7.27%, 7.62% for 0.60% volume fraction, and 7.62%, 8.44% for 1.18% volume fraction. The experimental data recorded 15.645% and 10.206% at 1.18% and 0.60% volume fractions of nanoparticles, respectively. In addition, the model presented by Vajjha *et al.* [10], Fig. 8, which include the Brownian motion influence and consider the behavior of heat transfer coefficient as a function of temperature, found to have the closest results after the mentioned models where the increase in

heat transfer coefficient is 10.353%, and 8.086% for 1.18% and 0.60% with standard deviation 10.45%, and 7.44%, respectively. The other used models such as for example due to He [20] shows more deviated results as noticed in Fig. 6, with standard deviation 10.39%, and 12.63 for 0.60%, and 1.18%, respectively. From the previous results, one can notice that the most consistency with experimental data was found using the models where the
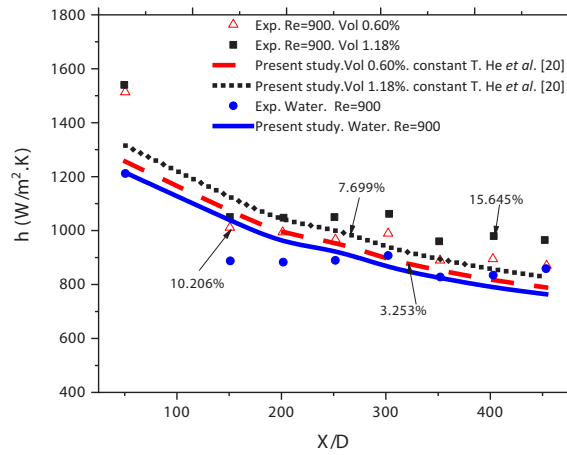

Figure 6: Axial profile for convective heat transfer coefficient achieved by applying He *et al.* model [20] at two volume fraction of nanoparticles in comparison with the experimental data.
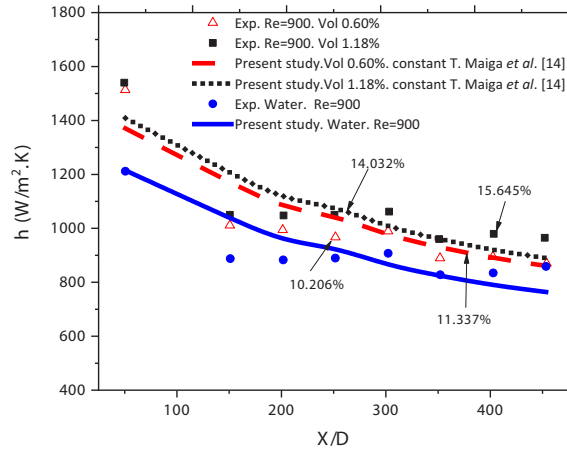
Figure 7: Axial profile for convective heat transfer coefficient achieved by applying Maiga *et al.* model [14] at two volume fraction of nanoparticles in comparison with the experimental data.

effect of temperature variation was not considered. The results presented in Figs. 4 and 5 accounting for the effective thermal conductivity and dynamic viscosity, exhibit the closest consistency with data obtained using the He model while the results of the heat transfer coefficient along the axial distance are consistent with Maiga, and Corcione, which can be obtained at the constant temperature 295 K that was used in the experiment
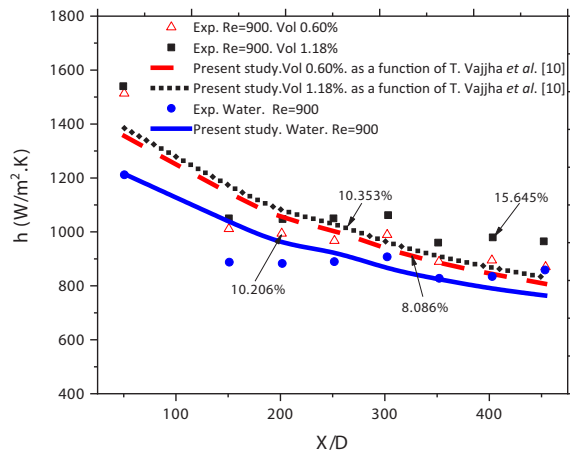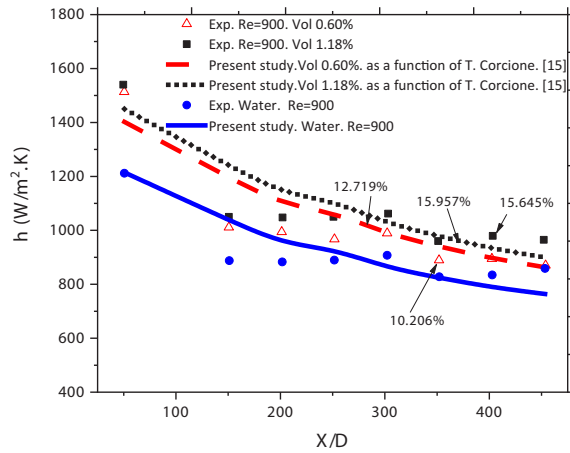

Figure 8: Axial profile for convective heat transfer coefficient achieved by applying Vajjha *et al.* model [10] at two volume fraction of nanoparticles in comparison with the experimental data.

Figure 9: Axial profile for convective heat transfer coefficient achieved by applying Corcione model [15] at two volume fraction of nanoparticles in comparison with the experimental data.

to predict the effective thermal properties and then to form the mentioned model in the case of Corcione model. The validity of the Maiga model for calculating the effective thermophysical properties that were used to predict the thermal conductivity, dynamic viscosity, specific heat capacity and density of the nanofluid in opposite to some models where they skip the effect of density and specific heat capacity. However neglecting the effect of the effective density has a large impact on the velocity field of the nanofluid, which is proportional inversely to the nanofluid fluid density at constant Reynolds number. The previous details explore the importance of considering the effect of temperature variation and all the effective thermophysical properties, which may affect the properties of nanofluids.

9.5   Nusselt number

Calculations for Nusselt number were also achieved using the presented models. It is shown that an improvement in Nusselt number with the nanoparticle concentration for all used models is observed despite the paradoxical recordings in amelioration percent in comparison among the considered models. However, the results were compared with experimental data of Nusselt number and best agreement was detected using the Corcione model [15], Fig. 10, which indicated 11.242% and 9.585% improvement for 1.18% and 0.60% volume fraction of nanoparticles, with standard deviation equal to 8.25%, and 7.60%. The experimental data registered 9.372%
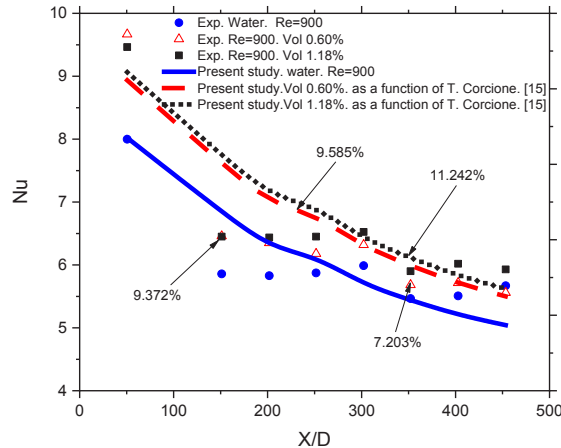

Figure 10: Axial profile for Nusselt number achieved by applying Corcione model [15] at two volume fraction of nanoparticles in comparison with the experimental data.

and 7.203% for 1.18% and 0.60% volume fraction of the nanoparticles, respectively. However, the next model, which has the closest agreement such as Corcione one is the Maiga model [14], Fig. 11, which recorded 11.213% and 9.874% for 1.18% and 0.60% volume fraction of the nanoparticles, with standard deviation equal to 7.88%, and 7.39%, respectively. From the previous results, the most suitable model for evaluating the effective properties of nanofluid, which satisfies appropriate results in comparison with experimental work, is the Corcione model, which includes essential parameters such as the effect of temperature variation, nanoparticle diameter impact on thermal conductivity and viscosity, the particle diameter of the base fluid used in the nanofluid, and the Boltzmann constant. Maiga model exhibit the same result, the model does not exhibit the temperature variation effect but indicates the effect of the four essential properties of the nanofluid, represented by thermal conductivity, dynamic viscosity, specific heat capacity, and density. The difference between the Corcione model and Maiga model is that the first one recorded higher values than the second one in comparison to the experimental values with almost the same deviation and this can be interpreted by values of the effective thermal conductivities which were found by every model that is proportionally inverse with the Nusselt number. Vajjha model Fig. 12, exhibits more deviated results, which affected by the effective thermal conductivity and by its role control the outcomes of Nusselt number in comparison to the experimental and other presented models, as discussed before. Also, it observed that the effective thermal
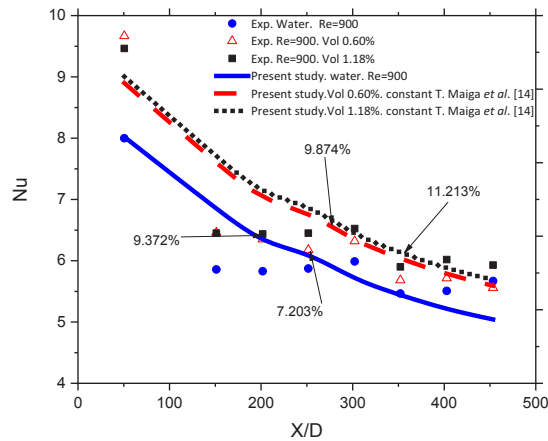

Figure 11: Axial profile for Nusselt number achieved by applying Maiga *et al.* model [14] at two volume fraction of nanoparticles in comparison with the experimental data.

conductivity and effective dynamic viscosity is showing the best agreement with He (Figs. 3 and 4), while it has a high deviation in detecting the Nusselt number as shown in Fig. 13, which can be interpreted similarly by the importance of the effective density effect which affects the heat transfer coefficient and the Nusselt number through it and by the effective thermal conductivity which gives a different value by each model and is proportion-
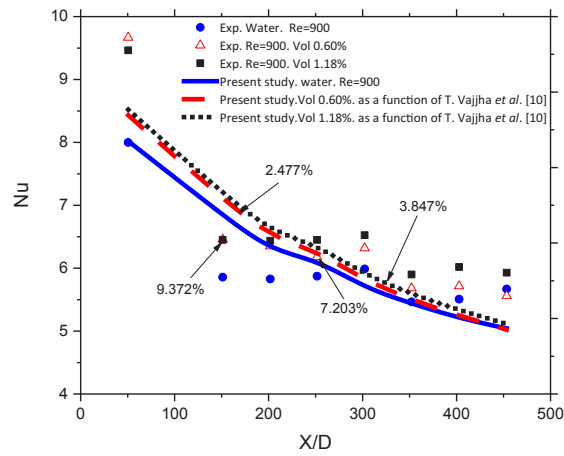

Figure 12: Axial profile for Nusselt number achieved by applying Vajjha *et al.* model [10] at two volume fraction of nanoparticles in comparison with the experimental data.
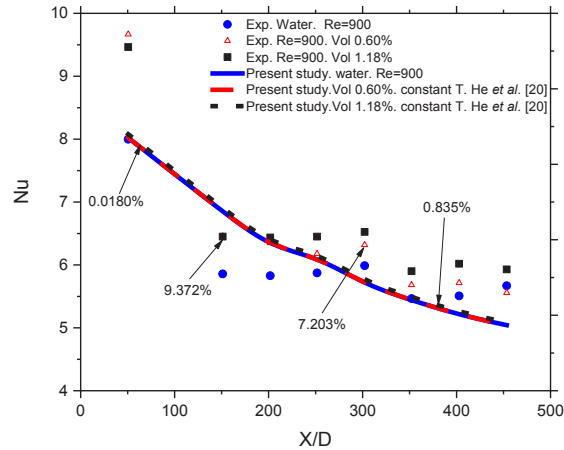

Figure 13: Axial profile for Nusselt number achieved by applying He *et al.* model [20] at two volume fraction of nanoparticles in comparison with the experimental data.

ally inverse with the Nusselt number. The standard deviations associated with Vajjha and He are 8.67%, 10.39%, and 10.31%, 12.63% for 0.60%, and 1.18% volume fraction, respectively.

9.6 Radial profiles of velocity

The radial profiles of velocity at different axial positions have been determined and shown in Fig. 14. They were measured at two values of volume fractions of nanoparticles, constant heat flux of 4000 W/m^2, and fixed Reynolds number of 900. Various results were recorded according to the used models. The first model of Vajjha *et al.* [10] recorded the maximum velocity in the center of the pipe and was reducing gradually with approach to the walls. That is an expected result as the mentioned behavior is a general case for laminar flow considered in the present study, Figs. 14–16, for water and nanofluids at different concentrations. On the other hand, the velocity field for the base fluid higher than the velocity of nanofluid and reduced with increasing the volume fraction of the nanoparticles along with the various positions of the axial profiles. and this behavior is a result of the low effective dynamic viscosity as shown in Fig. 3, in comparison to the effective density found at a specific concentration of nanoparticles. However, the effective dynamic viscosity increased in comparison to the effective density with the rising in the nanoparticle concentration. The previous behavior is related to the mechanism found in Vajjha model, and as men-
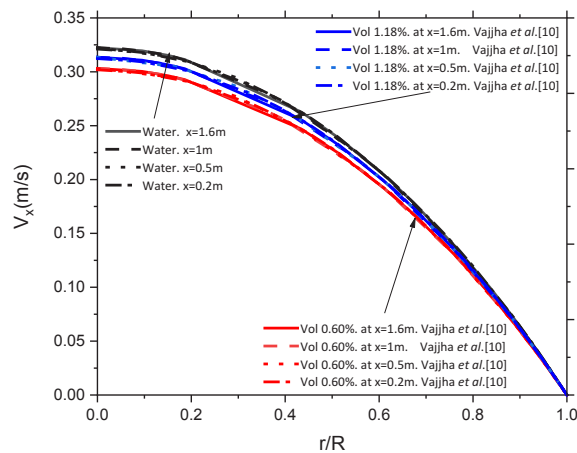

Figure 14: Axial profiles of local axil velocity Vajjha *et al.* model [10] at two volume fraction of nanoparticles in comparison with the experimental data.

tioned before that this the model designed to work in specific conditions, which may be considered as a reason to have such behavior (Fig. 14). Corcione [15] model and Maiga [14] models exhibit a similar behavior shown by reducing the velocity from the center towards the tube walls, but the behavior shows the increase in velocity with increase in the nanoparticle concentrations and this behavior is related to the increasing in the effective dynamic viscosity to the effective density at fixed Reynolds number (Figs. 15 and 16), as explained before.
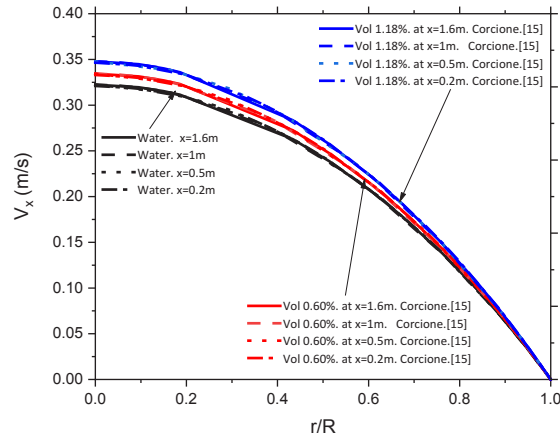

Figure 15: Axial profiles of local axil velocity Corcione model [15] at two volume fraction of nanoparticles in comparison with the experimental data.

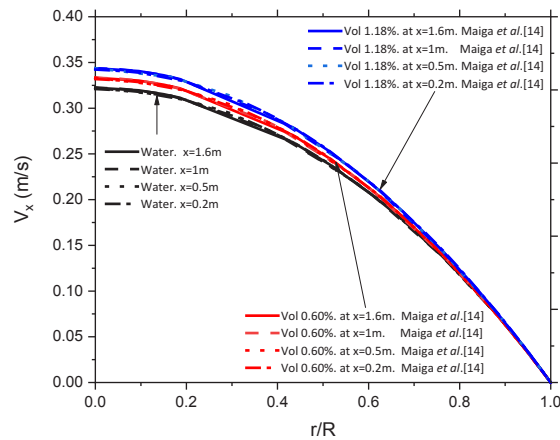Figure 16: Axial profiles of local axil velocity Maiga *et al.* model [14] at two volume fraction of nanoparticles in comparison with the experimental data.

9.7 Temperature distribution

Temperature distribution inside the pipe is shown in Figs. 17, 18, and 19, which present the effect of nanoparticles' addition on the temperature distribution using the presented models. In general, the temperature increases gradually from the center of the flow to the walls for all models. Vajjha model [10] determine the increase in temperature with the addition of
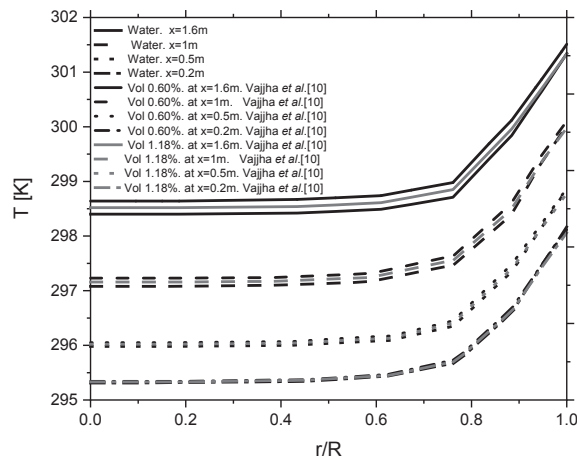

Figure 17: Temperature distribution in Vajjha *et al.* model [10] at two volume fraction of nanoparticles in comparison with the experimental data.
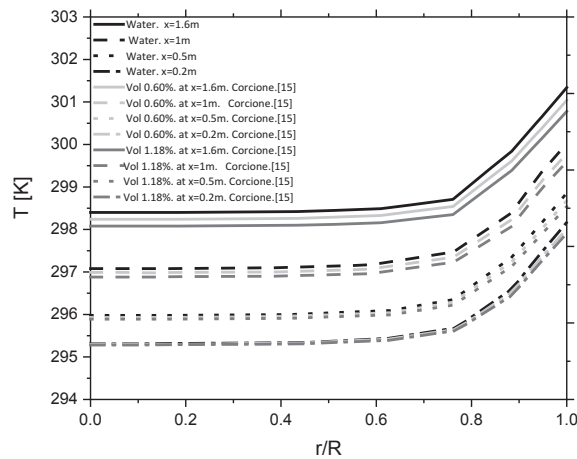

Figure 18: Temperature distribution in Corcione model [15] at two volume fraction of nanoparticles in comparison with the experimental data.

nanoparticles and the maximum improvement is found at 0.6% volume fraction and it reduces with the nanoparticles volume fraction raising to 1.18% (Fig. 17). This behavior can be connected with the velocity field effect, which was explained previously, that the reduction in the velocity of the nanofluid gives more time to transfer the heat from the supplied constant heat flux to the nanofluid. Corcione model [15] and Maiga models [14] (Figs. 18 and 19) exhibit the behavior, which agree with their velocity field, that the temperature distribution reduces with increasing the nanoparticles concentration as a result to their velocity field, which increases with the addition of nanoparticles, so there is less time to transfer the heat through the nanofluid.
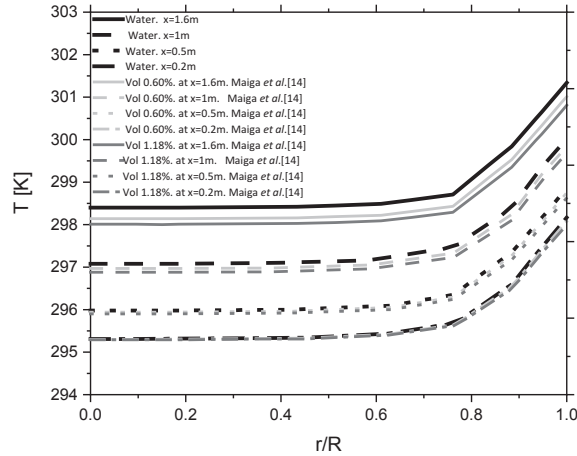

Figure 19: Temperature distribution in Maiga *et al.* model [14] at two volume fraction of nanoparticles in comparison with the experimental data.

10   Conclusions

Numerical simulation for the convective laminar flow inside a circular pipe supplied with the constant heat flux has been studied for the base fluid and nanofluid using different nanoparticle concentrations. The effect of nanoparticles added to the base fluid on the thermophysical properties, which affect the heat transfer coefficient and Nusselt number has been discussed by applying various models to account for the effective properties. Also, the velocity field and temperature distribution for the base fluid and nanofluid have been discussed. The comparison of the numerical results with experimental data was conducted using the presented models.

The results show that every model has a special mechanism to evaluate the effective properties that some models depend on the temperature variation and some of them are independent to the temperature variation. However, the temperature-dependent approaches can consider a valuable parameter that should be taken into account despite that independent on the temperature model can give good results in some cases. The closest results have been found at two models, one of them temperature-dependent and the other one independent of temperature.

The model should offer the posibility of evaluation of effective properties for the four essential parameters of nanofluids such as effective thermal conductivity, effective dynamic viscosity, effective density, and effective specific heat capacity, to give the right outcome for the presented case that effective dynamic viscosity and effective density are related directly to the velocity field of the nanofluid at constant Reynolds number. On the other hand the heat transfer coefficient, and thermal conductivity control the Nusselt number. Models that do not offer the change in the four mentioned parameters such as neglecting the effect of effective density will not give accurate results.

Nanoparticles addition improves effective thermal conductivity, heat transfer coefficient, and increases the effective dynamic viscosity to the effective density, which increases the velocity field of the nanofluid according to Corcione and Maiga models. For the Vajha model, the mechanism is different. The effective dynamic viscosity decreases at some nanoparticles ratio, which reduces the velocity but at the same time, the effective thermal conductivity increases in a sufficient amount to improve the heat transfer coefficient of the nanofluid with the addition of nanoparticles.

References

[1] MIRMASOUMI S., BEHZADMEHR A.: *Numerical study of laminar mixed convection of a nanofluid in a horizontal tube using two-phase mixture model.* Appl. Therm. Eng. **28**(2008), 7, 717–727.

[2] BIANCO V., MANCA O., NARDINI S.: *Numerical investigation on nanofluids turbulent convection heat transfer inside a circular tube.* Int. J. Therm. Sci. **50**(2011), 3, 341–349.

[3] MASUDA H., EBATA A., TERAMAE K.: *Alteration of thermal conductivity and viscosity of liquid by dispersing ultra-fine particles. Dispersion of Al_2O_3, SiO_2 and TiO_2 ultra-fine particles.* Netsu Bussei **7**(1993), 4, 227–233.

[4] Choi S.U.S., Eastman J.A.: *Enhancing thermal conductivity of fluids with nanoparticles.* Argonne National Lab., ANL/MSD/CP-84938, CONF-951135-29, 1995.

[5] Daungthongsuk W., Wongwises S.: *A critical review of convective heat transfer of nanofluids.* Renew. Sustain. Energy Rev. **11**(2007), 5, 797–817.

[6] Godson L., Raja B., Lal D.M., Wongwises S.: *Enhancement of heat transfer using nanofluids – an overview.* Renew. Sustain. Energy Rev **14**(2010), 2, 629–641.

[7] Pak B.C., Cho Y.I.: *Hydrodynamic and heat transfer study of dispersed fluids with submicron metallic oxide particles.* Exp. Heat Transfer **11**(1998), 2, 151–170.

[8] Eastman J.A.: *Novel thermal properties of nanostructured materials.* Argonne National Lab., ANL/MSD/CP-96711, 1999.

[9] Wen D., Ding Y.: *Experimental investigation into convective heat transfer of nanofluids at the entrance region under laminar flow conditions.* Int. J. Heat Mass Tran. **47**(2004), 24, 5181–5188.

[10] Vajjha R.S., Das D.K.: *Experimental determination of thermal conductivity of three nanofluids and development of new correlations.* Int. J. Heat Mass Tran. **52**(2009), 21-22, 4675–4682.

[11] Ebrahimnia-Bajestan E., Niazmand H., Duangthongsuk W., Wongwises S.: *Numerical investigation of effective parameters in convective heat transfer of nanofluids flowing under a laminar flow regime.* Int. J. Heat Mass Tran. **54**(2011), 19-20, 4376–4388.

[12] Lee S., Choi S.S., Li S.A., Eastman J.A.: *Measuring thermal conductivity of fluids containing oxide nanoparticles.* J. Heat Transf. **121**(1999), 2, 280–289.

[13] Wang X., Xu X., Choi S.U.S.: *Thermal conductivity of nanoparticle-fluid mixture.* J. Thermophys. Heat Tr. **13**(1999), 4, 474–480.

[14] Maiga S.E.B., Palm S.J., Nguyen C.T., Roy G., Galanis N.: *Heat transfer enhancement by using nanofluids in forced convection flows.* Int. J. Heat Fluid Fl. **26**(2005), 4, 530–546.

[15] Corcione M.: *Empirical correlating equations for predicting the effective thermal conductivity and dynamic viscosity of nanofluids.* Energ. Convers. Manage. **52**(2011), 1, 789–793.

[16] Onyiriuka E.J., Obanor A.I., Mahdavi M., Ewim D.R.E.: *Evaluation of single-phase, discrete, mixture and combined model of discrete and mixture phases in predicting nanofluid heat transfer characteristics for laminar and turbulent flow regimes.* Adv. Powder Technol. **29**(2018), 11, 2644–2657.

[17] Bianco V., Chiacchio F., Manca O., Nardini S.: *Numerical investigation of nanofluids forced convection in circular tubes.* Appl. Therm. Eng. **29**(2009), 17–18, 3632–3642.

[18] Moraveji M.K., Ardehali R.M.: *CFD modeling (comparing single and two-phase approaches) on thermal performance of Al_2O_3/water nanofluid in mini-channel heat sink.* Int. Commun. Heat Mass **44**(2013), 157–164.

[19] Vanaki S.M., Ganesan P., Mohammed H.A.: *Numerical study of convective heat transfer of nanofluids: a review.* Renew. Sustain. Energy Rev. **54**(2016), 1212–1239.

[20] He Y., Men Y., Zhao Y., Lu H., Ding Y.: *Numerical investigation into the convective heat transfer of TiO_2 nanofluids flowing through a straight tube under the laminar flow conditions.* Appl. Therm. Eng. **29**(2009), 10, 1965–1972.

[21] Khanafer K., Vafai K.: *A critical synthesis of thermophysical characteristics of nanofluids.* Int. J. Heat Mass Tran. **54**(2011), 19-20, 4410–4428.

[22] Koo J., Kleinstreuer C.: *A new thermal conductivity model for nanofluids.* J. Nanopart. Res. **6**(2004), 6, 577–588.

[23] Kim D., Kwon Y., Cho Y., Li C., Cheong S., Hwang Y., Moon S.: *Convective heat transfer characteristics of nanofluids under laminar and turbulent flow conditions.* Curr. Appl. Phys. **9**(2009), 2, 119–123.

[24] Mcnab G.S., Meisen A.: *Thermophoresis in liquids.* J. Colloid Inter. Sci. **44**(1973), 2, 339–346.

[25] Shah R.K.: *Laminar Flow Forced Convection in Ducts. Academic Press*, A.L. London, New York, 1978. p.128.

[26] https://www.comsol.com/release/5.4 (accessed: 20 May 2020).